Received: 23 March 2021 | Revised: 27 April 2021 | Accepted: 30 April 2021

DOI: 10.1002/ardp.202100111

FULL PAPER

ARCH PHARM DPhG
Archiv der Pharmazie

Silver–*N*-heterocyclic carbene complexes-catalyzed multicomponent reactions: Synthesis, spectroscopic characterization, density functional theory calculations, and antibacterial study

Aziza Mnasri[1,2] | Amal Mejri[1] | Sadok M. Al-Hazmy[3] | Youssef Arfaoui[4] | Ismail Özdemir[2,5] | Nevin Gürbüz[2,5] | Naceur Hamdi[1,6]

[1]Research Laboratory of Environmental Sciences and Technologies (LR16ES09), Higher Institute of Environmental Sciences and Technology, University of Carthage, Tunis, Tunisia

[2]Catalysis Research and Application Center, İnönü University, Malatya, Turkey

[3]Department of Chemistry, College of Science, Qassim University, Buraidah, Saudi Arabia

[4]Laboratory of Characterizations, Applications & Modeling of Materials (LR18ES08), Department of Chemistry, Faculty of Sciences, University of Tunis El Manar, Tunis, Tunisia

[5]Department of Chemistry, Faculty of Science and Art, İnönü University, Malatya, Turkey

[6]Department of Chemistry, College of Science and Arts, Qassim University, Ar Rass, Saudi Arabia

Correspondence
Naceur Hamdi, Research Laboratory of Environmental Sciences and Technologies (LR16ES09), Higher Institute of Environmental Sciences and Technology, University of Carthage, Hammam-Lif, Tunisia, PB 77-P.O. Box 77, 1054 Amilcar, Tunisia.
Email: naceur.hamdi@isste.rnu.tn

Abstract

Nowadays, silver–*N*-heterocyclic carbene (silver–NHCs) complexes are widely used in medicinal chemistry due to their low toxic nature toward humans. Due to the success of silver–NHCs in medicinal applications, interest in these compounds is rapidly increasing. Therefore, the interaction of *N*,*N*-disubstituted benzimidazolium salts with Ag_2O in dichloromethane to prepare novel Ag(I)–NHCs complexes was carried out at room temperature for 120 h in the absence of light. The obtained complexes were identified and characterized by ^{1}H and ^{13}C nuclear magnetic resonance, Fourier-transform infrared, UV–Vis, and elemental analysis techniques. Then, the silver complexes were applied for three-component coupling reactions of aldehydes, amines, and alkynes. The effect of changing the alkyl substituent on the NHCs ligand on the catalytic performance was investigated. In addition, it has been found that the complexes are antimicrobially active and show higher activity than the free ligand. The silver–carbene complexes showed antimicrobial activity against specified microorganisms with MIC values between 0.24 and 62.5 μg/ml. These results showed that the silver–NHC complexes exhibit an effective antimicrobial activity against bacterial and fungal strains. A density functional theory calculation study was performed to identify the stability of the obtained complexes. All geometries were optimized employing an effective core potential basis, such as LANL2DZ for the Ag atom and 6-311+G(d,p) for all the other atoms in the gas phase. Electrostatic potential surfaces and LUMO–HOMO energy were computed. Transition energies and excited-state structures were obtained from the time-dependent density functional theory calculations.

KEYWORDS

antimicrobial activity, antitumor activity, benzimidazolium salt, DFT calculations, multicomponent reactions, silver catalysis, structural characterization

1 | INTRODUCTION

N-Heterocyclic carbenes (NHCs) are neutral two-electron donors and are known to be strong Lewis bases and excellent nucleophiles that bind metals better than phosphines.[1] NHCs have been widely studied for their intriguing structural properties. Since then, the number of studies in this area have increased considerably. NHCs have emerged as an important building block in coordination chemistry. Due to their good σ-donating property, NHCs form bonds with metals at a greater stability than phosphines, and the lone pair of electrons on the carbene carbon, and they are stabilized by adjacent nitrogen atoms via inductive effect.[2–6] The variability of the biological activities of NHCs greatly depends on the ring size and structure of the substitutions over the ring.[7–9] In 1944, Wooley[10] reported that benzimidazole can act similarly as purines. Following that study, it was demonstrated that benzimidazole derivatives possess several biological activities, such as antihypertensive, anti-inflammatory, antimicrobial, antiviral, antioxidant, antitumor, lipid modulator, and anticoagulant activities.[11–13] Silver salts have historically been used as antimicrobial agents for the prevention of eye infections in newborns and the purification of drinking water, as well as in wound healing.[14,15] Also, it is clear that the number of silver centers plays a crucial role in bioactivity. As the number of silver centers in a complex increases, the concentration of Ag^+ ions in target site also increases. This enhances the cytotoxicity of the complex. The presence of lipophilic groups such as alkyl chains on NHC ligand increases the lipophilic nature of the complex, which helps easy penetration of the complex into the cell wall. On the contrary, the disadvantage of existing well-known silver-based drugs is that they lose their effects rapidly due to the quick release of the Ag^+ ions. Therefore, the synthesis of silver complexes having strongly coordinating ligands such as NHCs is very important for medicinal applications.[16] Propargylamines were prepared by the addition of a metal acetylide to an imine group.[17] However, this traditional method has some drawbacks, such as the use of stoichiometric amounts of strong bases and the high moisture sensitivity of the organometallic reagents formed. The metal-catalyzed coupling reaction of aldehydes, amines, and alkynes (A^3 coupling) to give propargyl amines has been improved in recent years.[18–20] The only by-product is water in this method, which is a one-pot multicomponent reaction. Most biomedical studies on silver–NHC complexes have been conducted concerning their antimicrobial properties.[21–25] Although the cytotoxic effects of silver compounds on bacteria have long been established, the mechanisms of action are not completely understood. Sporadic studies of the cell toxicity mechanisms of silver compounds suggest that silver ions kill organisms in a variety of ways.[26–30] In this area, many articles have been recently published on the synthesis and applications of silver–NHC complexes. Recently, we reported bio-organometallic studies of silver and gold complexes of imidazolin-2-ylidene and benzimidazole-2-ylidene ligands for antimicrobial applications.[31–35] The presence of a strong metal–ligand bond has attracted the attention of medicinal chemists toward the anticancer activity of Ag–NHC complexes.[36] A mini-review by Tacke et al. covered the anticancer and antibiotic activities of benzyl-substituted metal–NHC complexes.[37] Recently, a review by Hecel focused on antimicrobial and anticancer applications of silver complexes as potential therapeutic agents. Hecel's review also summarized the pharmacological applications of Ag^+ nanoparticles in medicine and pharmacy.[38] Also, it is seen that the number of studies in the field of examining the antimicrobial properties of silver–NHCs against bacteria and fungi is increasing rapidly.[39] Here, we describe the synthesis, characterization, and antimicrobial applications of new silver complexes containing unsymmetrical NHC ligands. The structures of all silver–NHC complexes were characterized by elemental analysis as well as by ^1H nuclear magnetic resonance (NMR), ^{13}C NMR, and infrared (IR) spectroscopic techniques. The silver complexes were applied in three-component coupling reactions of aldehydes, amines, and alkynes. In addition, the antimicrobial activities of these complexes were tested against Gram-negative bacteria, Gram-positive bacteria, and fungi. We show that these new silver–NHC complexes are efficient antimicrobial agents against different microorganisms. Density functional theory (DFT) and time-dependent density functional theory (TD-DFT) calculations were reported to carry out correlations between experimental and theoretical parameters and physical properties.

2 | RESULTS AND DISCUSSION

2.1 | Preparation and structural properties of benzimidazolium salts 2a–f

Target benzimidazole salts **2a–f** were achieved via a two-step *N*-alkylation process, as depicted in Scheme 1. The first step involves the addition of an *N*-alkyl chlorane group in the presence of KOH in dimethyl sulfoxide (DMSO) at 80°C for 72 h to the corresponding benzimidazole or 5,6-dimethylbenzimidazole, enhancing the reactivity of the other nitrogen atom. The addition of the appropriately substituted benzyl chloride in dimethylformamide (DMF) at 80°C for 72 h to the remaining nitrogen atom gives desired *N*,*N*′-disubstituted benzimidazolium salts **2a–f**. The salts obtained were soluble in polar solvents such as methanol, ethanol, DMSO, and DMF but remained insoluble in nonpolar solvents such as diethyl ether, dichloromethane, and chloroform. Salts **2a–f** were stable in air and moisture environments in the solid state and in solution. Benzimidazolium salts **2a–f** were characterized by Fourier-transform infrared (FTIR) spectroscopy, ^1H and ^{13}C NMR spectroscopy, and elemental analysis.

The FTIR spectroscopy, ^1H and ^{13}C NMR spectroscopy, and elemental analysis data of the title compounds confirm the proposed structures. NMR spectra of all the compounds were analyzed in $CDCl_3$. In the ^1H NMR spectra, acidic protons (NCHN) for benzimidazolium salts **2a–f** were observed at 11.00, 11.21, 10.63, 11.08, 11.19, and 11.09 ppm, respectively, as characteristic sharp singlets. In the ^{13}C NMR spectra of benzimidazole salts **2a–f**, the NCHN carbon was detected as typical singlets at 143.2, 143.3, 143.7, 143.8,

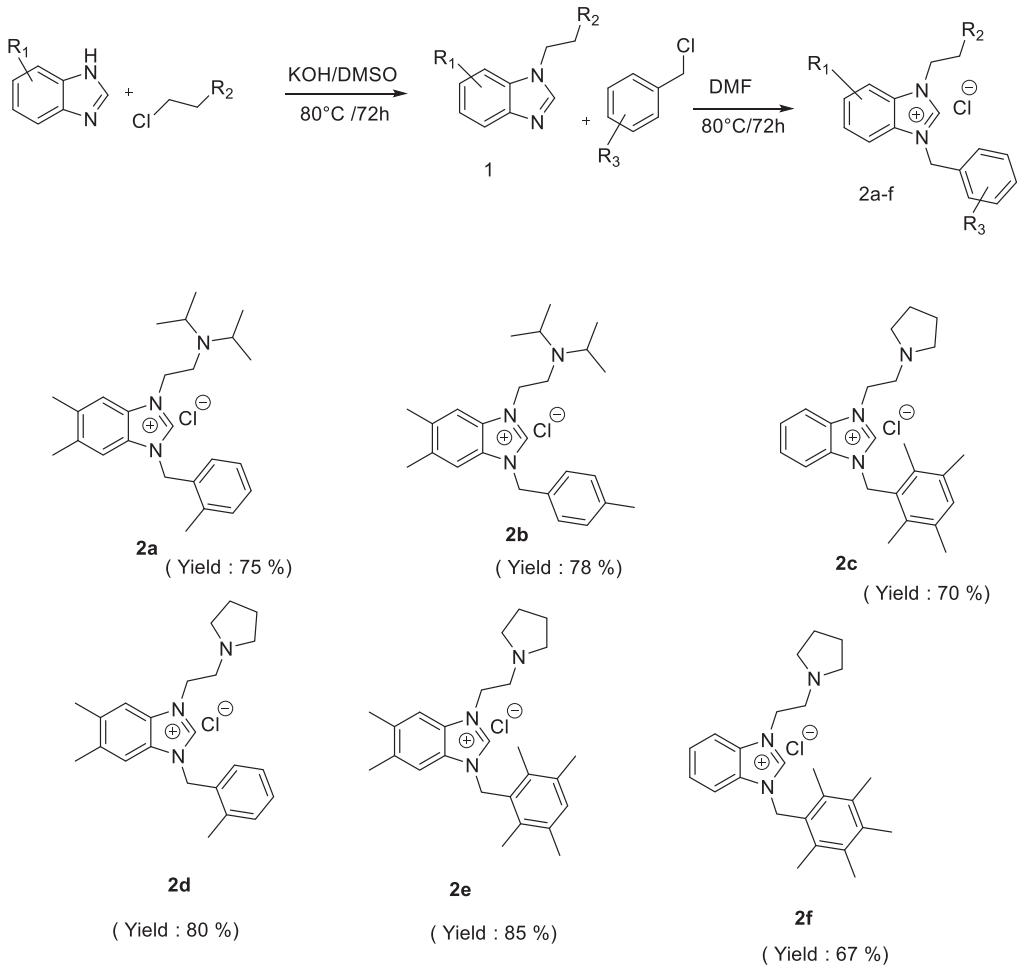

SCHEME 1 General synthesis and structure formulas of 1,3-dialkylbenzimidazolium salts **2a**–**f**. DMF, dimethylformamide; DMSO, dimethyl sulfoxide

141.6, and 143.1 ppm. In the IR spectra, ν(C=N) bands for salts **2a**–**f** were observed at 1549, 1550, 1559, 1558, 1560, and 1560 cm^{-1}. Aromatic protons of benzimidazolium salts **2a**–**f** were detected in the range of 7.01–8.02 ppm. Methyl protons of the isopropyl group on all benzimidazolium salts were seen as doublets in the range of 0.75–0.76 ppm. N–CH– protons of the isopropyl group on benzimidazolium salts **2a**–**f** resonated between 2.04 and 2.06 as multiplets; however, methylic protons $-CH_2-N$ of benzimidazolium salts **2a**–**f** signaled at 2.88–4.54 ppm as triplets. Methylic protons of pyrrolidine and piperidine groups on benzimidazolium salts (**2c**–**f**) resonated between 1.28 and 3.03 as multiplets; however, methylic protons $-CH_2-N$ of benzimidazolium salts (**2c**–**f**) signaled at 2.72–5.01 ppm as triplets. In the ^1H NMR spectra of (**2a**–**f**), $H_{1''}$ protons were detected as typical singlets between 5.47 and 5.82 ppm. The Ag–NHC complexes (**3a**–**f**) were prepared by in situ deprotonation of corresponding benzimidazolium salts (**2a**–**f**) using silver(I) oxide as the both metal source and base. The reactions were carried out in the dark in the presence of dichloromethane as the solvent at room temperature for 120 h, and the target complexes were obtained as white solids between 65% and 85% yields (Scheme 2). Complex **3** is an air-stable solid soluble in acetone, chloroform, dichloromethane, DMF, DMSO, ethanol, and acetonitrile, and insoluble in hexane, ether, and benzene.

The structure of the silver complexes was elucidated by NMR spectroscopy. In addition, it was also supported with FTIR spectroscopy and elemental analysis data. However, an attempt was made to obtain a single crystal for X-ray diffraction, but a suitable single crystal could not be obtained from these new silver complexes for X-ray diffraction. NMR spectra of all the compounds were analyzed in d-$CDCl_3$. In the ^1H NMR spectra of Ag(I)–NHC complexes **3a**–**f**, the acidic proton (NCHN) for NHC ligands (**2a**–**f**) was not observed, and its absence is proof of the formation of complexes **3a**–**f**. The characteristic signals (NCN) on the Ag(I)–NHC complexes **3a**–**f** were not detected exactly, which has also been mentioned in the literature and is a reason for the fluctuating behavior of NHC complexes.[40] These values are in agreement with reported data for similar Ag(I)–NHC complexes.[41] Aliphatic $-CH_2-$ protons of benzyl substituents for benzimidazolium salts were detected as a singlet at δ = 4.54–5.77 ppm. ^{13}C NMR chemical shifts provide a useful diagnostic tool for Ag–carbene complexes. In the ^{13}C NMR spectra of Ag–NHCs, characteristic signals of C(2) carbon of benzimidazolium salts **2a**–**f** completely disappeared. In our case for the complexes

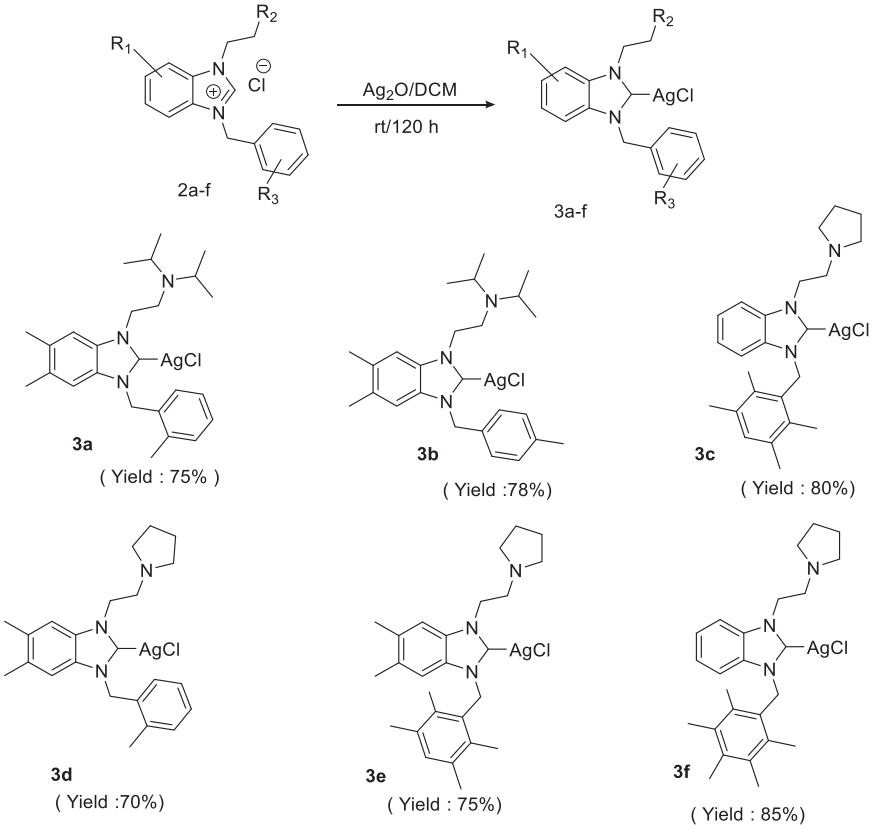

SCHEME 2 General synthesis and structure formulas of silver(I)–NHC complexes (**3a–f**). DCM, dichloromethane; NHC, *N*-heterocyclic carbene

3a–f, the resonances for AgC(carbene) bond were not observed, which has also been mentioned in the literature and given as a reason for the fluxional behavior of the Ag–NHCs.[40–42] In the FTIR spectra, benzimidazole ring C=N vibrations of NHC ligands (**2a–f**) showed peaks at 1549, 1549, 1559, 1558, 1560, and 1560 cm^{-1}, respectively. After the formation of the complexes, C=N vibrations of Ag–NHC complexes **3a–f** shifted to lower energy regions, such as 1484, 1445, 1473, 1486, 1474, and 1478 cm^{-1}, respectively. This negative shift was attributed to the electropositive metal center, which pulls electron density toward itself. Also, elemental analysis data of the Ag–NHC complexes were consistent with the expected structures. A lot of work has been done by many groups on these types of complexes, which are extremely stable in air and moisture. Nolan and co-workers also showed that silver N-heterocyclic carbenes are a powerful catalysts.[43,44] Also, some days later, when the NMR of the solution in the NMR tube was taken again, the same NMR spectrum had been observed.

2.2 | UV–vis

The complex **3a** in chloroform shows a clear strong absorbance at 241 nm, due to the spin-allowed $S_0 \rightarrow S_2$ transition. The medium intensity longer wavelength bands at 286 nm indicate a spin-allowed $S_0 \rightarrow S_1$ transition. The lower intensity longer wavelength bands at 396 nm in chloroform and at 426 nm in ethanol are attributed to the spin-forbidden $S_0 \rightarrow T_1$ transition. Triplet state generation in the medium is enhanced by the heavy atom effect of silver ion. This explanation is supported by the higher absorbance at 286 nm and much higher at 241 nm in chloroform, which is a nonpolar solvent; Ag^+ is not solvated and exists near the emitting molecule, which causes more concentration of triplet state molecules, leading to higher absorbance that is confirmed by a clear increase in extinction coefficient values. The chlorine atoms represent heavy atoms on their own, as shown in Figure 1. It also shows the same behavior for complexes **3b** and **3c** with a 10-nm red shift in a spin-allowed $S_0 \rightarrow S1$ transition for complex **3c**.

The triplet state of complexes **3a–c** is not efficiently formed in acetonitrile; on the contrary, in a chloroform solvent, their

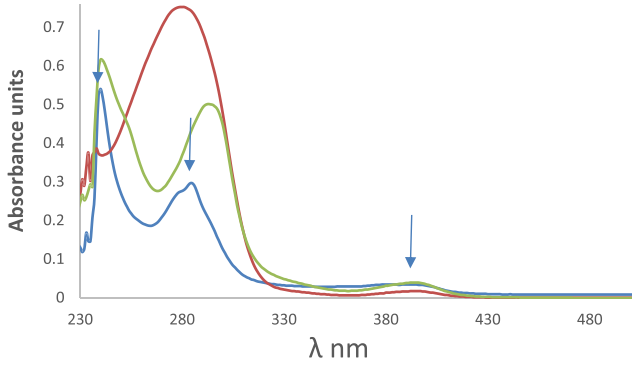

FIGURE 1 Absorption spectra of 1.5×10^{-4} M complexes (——) **3a**, (——) **3b**, and (——) **3c** in $CHCl_3$

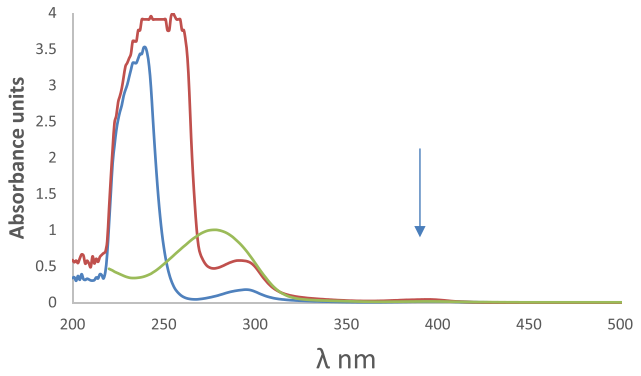

FIGURE 2 Absorption spectra of 1.5×10^{-4} M complexes (——) **3a**, (——) **3b**, and (——) **3c** in CH_3CN

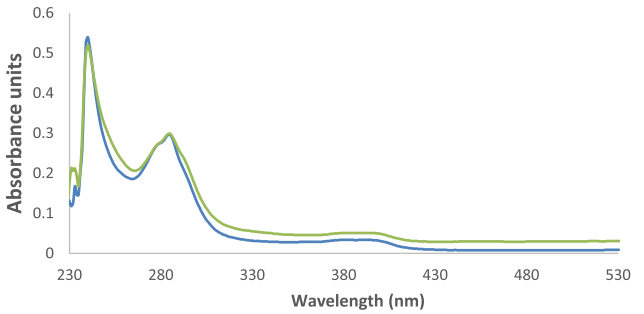

FIGURE 3 Absorption spectra of 3×10^{-5} ml/dm^3 of complex **3a** in $CHCl_3$ fresh (——) and irradiated solution (——) using 365-nm light for 24 h

absorbance in acetonitrile at 390 nm is negligible, as the values of the molar extinction coefficients are in the range 60–80 $M^{-1}{\cdot}cm^{-1}$, as shown in Figures 1 and 2 and Table 1, which may be attributed to the formation of a complex between acetonitrile and Ag^+.

Complex **3a** shows great optical stability, as no change in the emission and absorption spectra is observed on irradiation using 365-nm light for 24 h, as shown in Figure 3. Neither the acid nor the base affects the absorption spectra, as shown in Figure 4. An irregular Stokes shift was observed, which varied between 13, 42, and 91 nm in $CHCl_3$, CH_3CN, and ethanol of relative polarities, 0.460,

TABLE 1 Spectral data of complexes **3a–c**

Complex	Solvent	λ_{abs} max (nm)	λ_{em} max (nm)	ε ($M^{-1}{\cdot}cm^{-1}$)	ϕ_f	Solvent relative polarity
Complex **3a**	DMF	281		4337		0.386
		396	438	100		
	$CHCl_3$	285		1973		0.25
		396	438	220		
		482	595		0.10	
	CCl_4	395	433	2433	0.07	0.052
	Acetone	394	407	153		0.355
	i-Butanol	281		5631		0.552
		393	439	193		
	CH_3CN	280		2666		0.460
		396	409	100	0.03	
	Ethanol	292		2000	0.05	0.654
		427	519	206		
Complex **3b**	ETOH	392		1462		
	CH_3CN	396		85		
	DMF	394		4636		
Complex **3c**	ETOH	391	409	1277	0.02	
	Acetone	392	–	1325		
	C_4H_9Cl	390	–	795		
	Glycerol	390		1277		
	CH_3CN	396	409	80	0.02	
	$CHCl_3$		435			

Abbreviation: DMF, dimethylformamide.

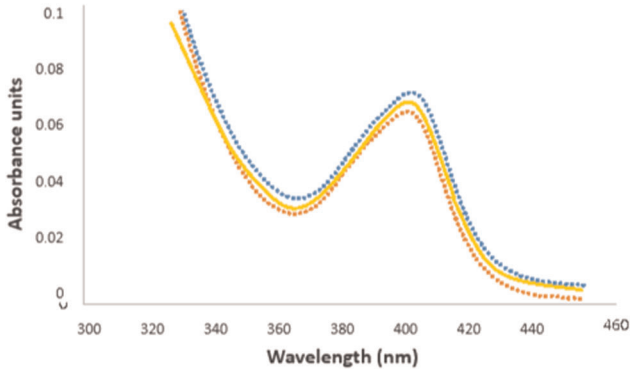

FIGURE 4 Absorption spectra of 3×10^{-5} ml/dm^3 of complex **3a** in CCl_4 fresh (▪▪▪▪), alkalized solution using triethylamine (———), and acidified solution using H_2SO_4 (▪▪▪▪)

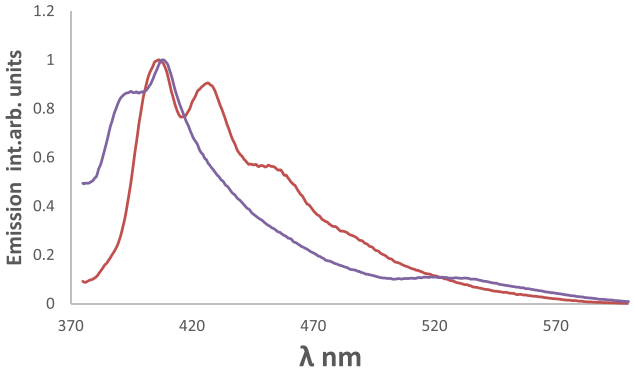

FIGURE 5 Normalized fluorescence spectra of 1.5×10^{-5} M complex **3a** in (———) acetone and (———) ethanol, λ_{ex} 365 nm

0.25, and 0.654, respectively, as shown in Table 1. In ethanol, the larger Stokes shift is due to better excited state solvation in such a polar solvent with the possibility of hydrogen bond formation. This is substantiated by the lack of vibrational structure of the emission spectrum of complex **3a** in ethanol in comparison to acetone, as indicated in Figure 5 and Table 1.

The difference between λ_{ex} max and λ_{ab} max of complex **3a** shown in Figure 6 is attributed to intramolecular proton transfer or rearrangement.

Table 1 also shows no change in λ_{abs} max. It seems that the ground states of complexes **3a–c** are not influenced by changing the relative solvent polarity and show a low molar absorptivity in the studied solvents.

Fluorescence was obtained only from complex **3a** in $CHCl_3$, CCl_4, ethanol, and CH_3CN at emission maxima wavelength, 595, 433, 519, 408, and 433 nm, respectively; λ_{ex} was at λ_{ab} max with a low fluorescence quantum yield (ϕ_f = 0.10, 0.08, 0.05, and 0.03, respectively). Emission spectra of complex **3a** in different solvents are shown in Figure 7. The blue shift in the maximum absorption wavelength of **3b** in ethanol as compared with acetonitrile, shown in Figure 8, is due to increase in solvent polarity.

2.3 | DFT calculations

All the calculations were performed via DFT using the Gaussian 09 set of programs.[45] The geometries of all products were optimized at the B3LYP level of theory. The calculations were performed employing an effective core potential basis, such as LANL2DZ for the Ag atom and 6-311+G(d,p) for all the other atoms.[46] Vibrational analyses confirmed that all products have zero imaginary frequencies. The electronic spectra were calculated using the TD-DFT.[47]

The frontier molecular orbitals, HOMO (highest occupied molecular orbital) and LUMO (lowest unoccupied molecular orbital), play an important role in several chemical processes. Thus, the larger the ε_{HOMO}, the greater is the electron-donating ability, and the smaller the ε_{LUMO}, the smaller is the resistance to accept electrons. Moreover, the energy gap ($\Delta\varepsilon$) between HOMO and LUMO characterizes the reactivity of the molecule. A molecule with a small $\Delta\varepsilon$ is more polarizable and generally associated with a high chemical reactivity.[48] HOMO and LUMO for complexes **3a–f** (Figure 9) were calculated from the optimized structure at the same level of theory.[49] It can be observed from Figure 10 and Table 2 that the HOMO in compounds **3a** and **3b** is mainly localized on the *N*-isopropylpropan-2-amine part, whereas for complex **3f** compounds, the HOMO is localized around the Cl site. The LUMO for complexes **3a**, **3b**, and **3f** is concentrated only in the benzimidazole moiety. $\Delta\varepsilon$ values for the obtained complex are summarized in Table 3.

The high $\Delta\varepsilon$ value in the case of complex **3a** refers to high chemical hardness and kinetic stability.[49] For the molecular electrostatic potentials (MEPs), it is seen that most of the negative potentials appear to be distributed on the Cl and N_{29} atoms (red color), whereas the positive potentials appear to be at N_8 and N_{10} atoms (blue color). In the MEP surface, red color refers to electron-rich (negative) region, blue color refers to electron-poor (positive) region, and green color signifies zero electrostatic potential. The charge distribution was similar in all studied complexes and was weakly influenced by the chemical environment (Figure 8 and Table 2).

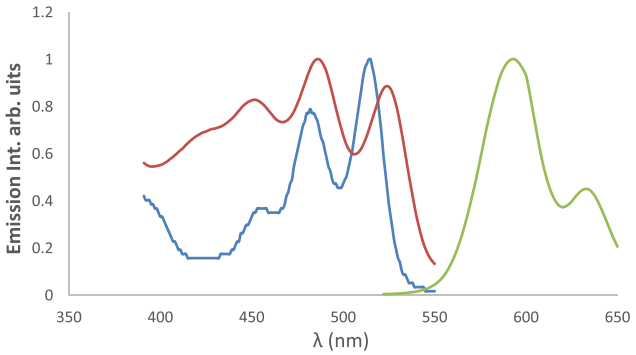

FIGURE 6 Normalized emission (———), excitation (———), and absorption (———) spectra of 1.5×10^{-4} M in $CHCl_3$

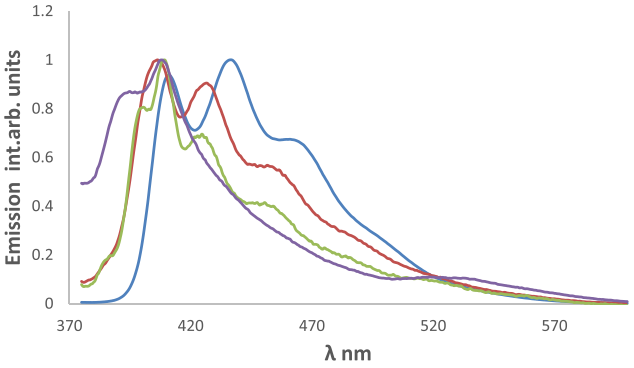

FIGURE 7 Normalized fluorescence spectra of 1.5×10^{-5} M complex **3a** in (——) $CHCl_3$, (——) CH_3N, (——) acetone, and (——) ethanol, λ_{ex} 365 nm

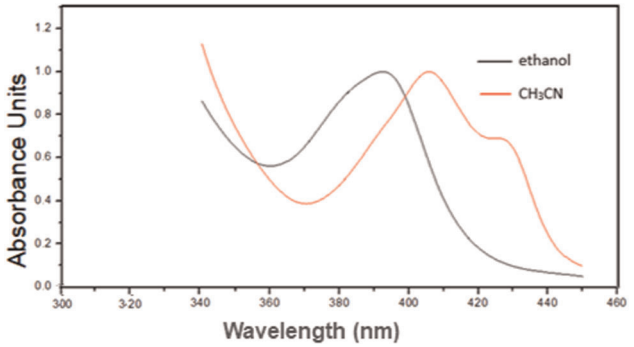

FIGURE 8 Normalized absorption spectra of complex **3b**, 6×10^{-4} mol/dm^3 in ethanol (▪▪▪▪) and 2.7×10^{-4} mol/dm^3 (——) in CH_3CN

To compare the experimentally obtained UV–visible and luminescence spectra with theoretical values, the TD-DFT method was applied to obtain a prediction of the emission spectra. Both theoretical emission and UV–visible spectra for **3a**, **3b**, and **3f** complexes are shown in Figures 11 and 12, respectively. The obtained spectra indicate relatively strong two-luminescence intensities with emission maxima at 315 and 375 nm for the **3a** complex, 314 and 366 nm for the **3b** complex, and 302 and 374 nm for the **3f** complex. This fluorescent maximum emission band can be attributed to the intraligand π*–π charge transitions of the benzimidazole moiety.[50] The calculated UV–visible spectra of complexes **3a**, **3b**, and **3f** display two intense bands centered at 262 and 312 nm for complex **3a**, two intense bands at 260 and 303 nm for **3b**, and two bands at 252nm and 307 nm for **3f** complexes, attributed to two π–π* transitions.

DFT calculations were adopted to investigate the geometry and spectral properties of the studied complexes. The obtained theoretical geometric parameters are approximately in good agreement with the experimental parameters (Figure 13 and Table 3), and there is approximately no effect of the substituent on the obtained geometric parameter results (Table 3).

2.4 | Catalytic activity of the silver(I)–NHC complexes (3a–f)

The three-component coupling reaction of alkynes, aldehydes, and amines catalyzed by transition metals is a useful approach for the preparation of propargyl amines as key intermediates in the building of nitrogen-containing biologically active compounds.[51] Transition metal complexes are efficient catalysts for this reaction.[52,53] However, there have been a limited number of reports related to the catalytic applications of NHC–Ag(I) complexes in A^3 coupling reactions.[54–56] In recent years, it has also been observed that silver compounds exhibit a highly effective catalytic activity for this three-component coupling reaction.[57] Herein, preliminary catalytic studies were carried out using phenylacetylene, piperidine, and *p*-formaldehyde at 80°C. The catalytic activity of complex **3** was examined in different solvents (Table 4, entries 1–5). Moderate yields were obtained in acetone and CH_3CN. A good catalytic activity was observed with complexes **3a**, **3c**, and **3f** under neat conditions (Table 4, entries 1 and 8). Whereas complexes **3b** and **3e** bearing different substituents on the NHC ligand showed similar activities (Table 4, entries 6, 13, and 17), lower yields were obtained by complex **3e** (Table 4, entries 14 and 18). It was concluded that the methyl group in compound **3g** caused a decrease in activity as compared with complex **3a**. It was previously reported that increasing the number of groups on the NHC ligand led to a decrease in activity.

A tentative mechanism was proposed involving the exchange of H of the C–H bond of alkyne by an Ag(I) species. The silver acetylide intermediate thus generated reacted with the iminium ion generated in situ from aldehydes and secondary amines to give the corresponding propargylamine and regenerate the Ag(I) catalyst for further reactions (Scheme 2).

Herein, according to the mechanistic studies reported in the literature regarding "A^3 coupling" reactions, we proposed a likely mechanism for the synthesis of propargylamines in the presence of **3**. In the first step of the catalytic cycle, a metal–acetylide intermediate is created. The formation of this intermediate renders the alkyne proton more acidic, causing its abstraction by iminium ion. Then, in situ generated metal acetylide reacts with iminium ion to provide propargylamine product and metal ion (Scheme 3).

It is well known that silver ions and silver-based compounds are highly toxic to microorganisms[58] and show strong biocidal effects; therefore, as an advancement of our previous studies, we now investigate the antimicrobial activity of the synthesized silver–NHC complex **3**.

2.5 | Antibacterial and antifungal activities

Ag–NHC complexes **3a–f** and salts **2a–f** were initially tested against bacterial strains with ampicillin and nystatin as standard drugs using the agar disc diffusion technique. In this section, the antimicrobial activities of Ag–NHC complexes **3a–f** and salts **2a–f** are described against *Listeria monocytogenes*, *Escherichia coli*, *Pseudomonas aeruginosa*, *Salmonella typhimurium*, and *Candida albicans*. The antimicrobial

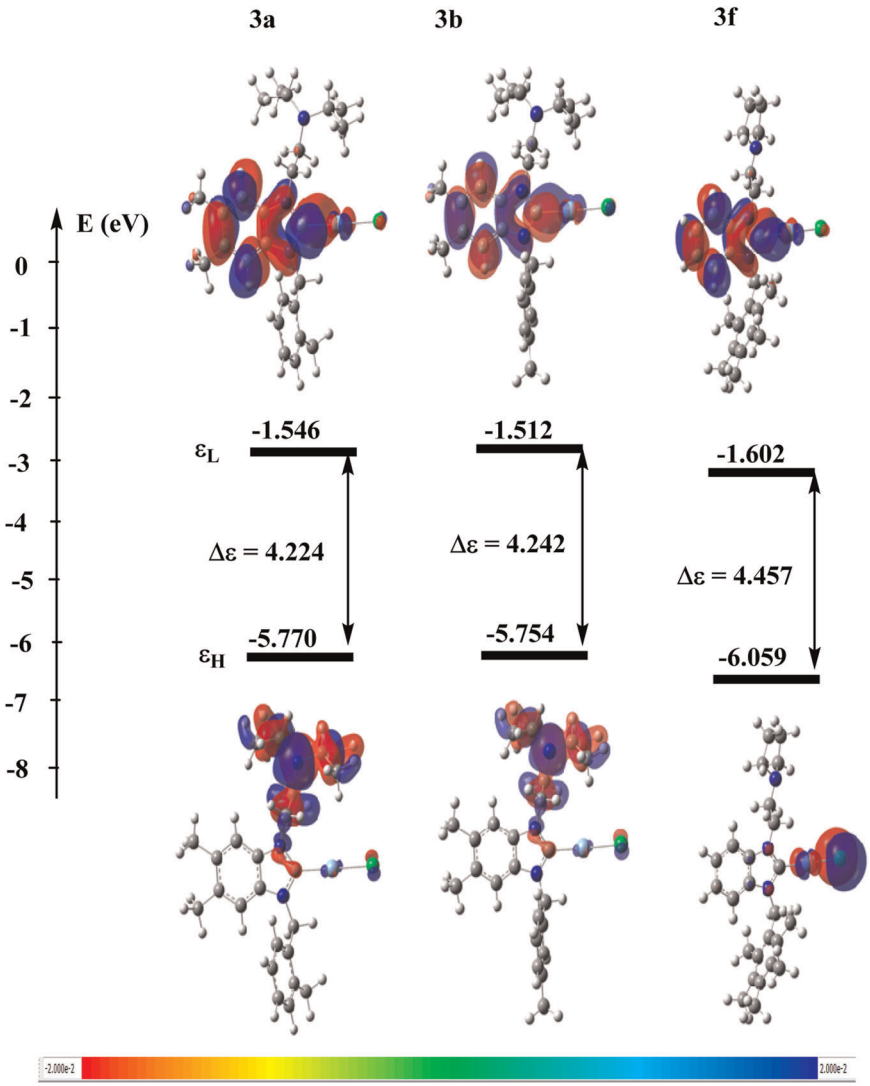

FIGURE 9 The calculated energies (eV) of the LUMO (L), HOMO (H), Δε, and plots of the calculated frontier molecular orbitals at isovalue = 0.02 a.u. of complexes **3a**, **3b**, and **3f**. The positive (blue) and negative (red) phase distributions in molecular orbital wave function. HOMO, highest occupied molecular orbital; LUMO, lowest unoccupied molecular orbital

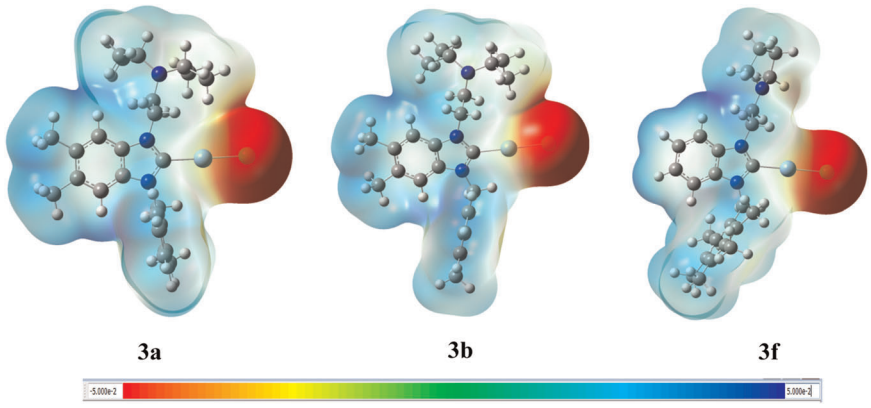

FIGURE 10 Molecular electrostatic potentials surface of the three complexes **3a**, **3b**, and **3f** mapped on the electron density isovalue of 0.0004 a.u

activity of these complexes, measured based on a zone of inhibition (zoi) parameter, is listed in Table 5, whereas the minimum inhibitory concentration (MIC) is listed in Table 6. When tested against bacteria at concentrations of 200–50 μg/ml, the silver–NHC complexes showed antibacterial activity. It was found that all complexes showed high levels of activity against Gram-negative and Gram-positive bacteria. It is interesting to note that *S. typhimurium* was not sensitive to the silver complex **3d** and salt **2c**. Complexes **3c** and **3b** showed higher activity (zoi = 31 mm and zoi = 25 mm, respectively) against *Staphylococcus aureus* (Table 5). Likewise, the corresponding MIC values of each of these two complexes were 0.24 and 3.9 mg/ml, respectively. The other benzimidazole salt **2** was inactive.

TABLE 2 Values of local minimum and maximum electrostatic potential ($V_{s,min}$ and $V_{s,max}$ in kcal/mol) of complexes **3a**, **3b**, and **3f** obtained at the electron density isosurface value of 0.0004 au

	Complex 3a		Complex 3b		Complex 3f	
	$V_{s,min}$ (kcal/mol)	$V_{s,max}$ (kcal/mol)	$V_{s,min}$ (kcal/mol)	$V_{s,max}$ (kcal/mol)	$V_{s,min}$ (kcal/mol)	$V_{s,max}$ (kcal/mol)
N_8		11.41		7.25		10.22
N_{10}		8.92		6.85		8.81
N_{19}	−6.77		−7.02		−10.99	
Cl	−44.02		−44.23		−44.35	

TABLE 3 ε_{HOMO}, ε_{LUMO}, $\Delta\varepsilon$ (eV), and geometric data of the **3a**–**f** complexes

Complexes	3a	3b	3c	3d	3e	3f
ε_{HOMO} (eV)	−5.770	−5.754	−6.082	−6.021	−6.019	−6.059
ε_{LUMO} (eV)	−1.546	−1.512	−1.635	−1.574	−1.470	−1.602
$\Delta\varepsilon$ (eV)	4.224	4.242	4.447	4.447	4.549	4.457
dAg–Cl (Å)	2.368	2.369	2.367	2.367	2.368	2.367
dC–Ag (Å)	2.119	2.119	2.123	2.120	2.122	2.123
dC_9–N_8 (Å)	1.362	1.362	1.361	1.362	1.361	1.361
dC_9–N_{10} (Å)	1.360	1.360	1.359	1.360	1.359	1.358
CÂgCl (°)	177.72	178.79	179.34	178.02	179.36	179.44
$\bar{\nu}$(Ag–Cl) (cm^{-1})	316.0	315.9	317.5	317.8	316.0	316.8

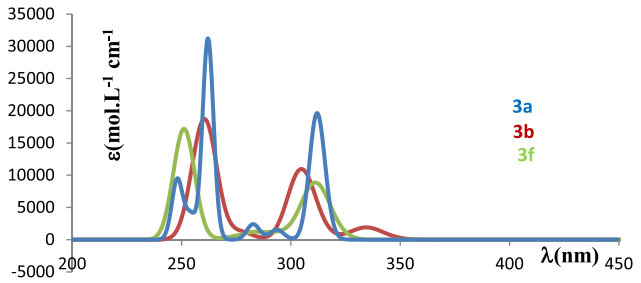

FIGURE 11 Luminescence spectra of the **3a**, **3b**, and **3f** complexes

Furthermore, it may be noted that the activity of the present complexes was better than that of the previously reported silver nitrate complexes.[59] The microorganism *C. albicans* was found to be sensitive to all of the salts **2** and their complexes studied **3**, with an activity varying in the range of 16–28 mm (zoi). Complex **3c** and salt **2c** showed the highest activities of 28 and 24 mm, respectively, against *C. albicans*.

To determine the efficacy of the complexes, MICs are determined. The MIC is the minimum concentration of compound necessary to inhibit the growth of a bacterial strain. A preliminary study of silver complex **3** was done to determine its MIC. The results of this compound were compared with that of silver nitrate, which was used as a positive control based on its established antimicrobial properties.[24]

The compounds were incubated for 24 h with the nonvirulent strains of *P. aeruginosa*, *S. aureus*, and *E. coli* in growth media.

Complex **3** showed antimicrobial activity at the concentrations tested (Table 6). Although there is evidence of silver complexes that have shown antimicrobial activity,[25,26] the results from the study of silver complex **3** are consistent with studies on other silver carbene complexes (SCCs) synthesized in our research group in which antimicrobial activity is observed.[12,15,16] The silver complexes **3c** and **3a**, however, showed inhibition of bacterial growth with MICs of 0.24 and 1.95 mg/ml, respectively, against *L. monocytogenes* ATCC 19117 and *S. typhimurium* ATCC 14028. These values were comparable to the MIC of silver nitrate (42.5 mg/ml), indicating that these new silver complexes are equally effective. Complex **3c** showed better activity than ampicillin against *Micrococcus luteus* with an MIC of 0.0025 mg/ml, whereas an MIC of 0.0045 mg/ml was observed in the case of *S. typhimurium* for complex **3c**. The MICs of other compounds remained within the tested range. Further studies are necessary to determine the efficacy of these compounds, compared with other SCCs, and their effectiveness against more virulent strains, but preliminary results demonstrate the potential of **3** in the treatment of bacterial infections.

3 | CONCLUSIONS

Five benzimidazolium salts and their Ag(I)–NHC complexes were synthesized using appropriate methods. The combination of FTIR, ^{1}H, and ^{13}C NMR spectral and elemental analyses suggested the formation of these complexes. The in vitro antimicrobial activities of the silver complexes were studied against four bacteria and two fungi to determine their inhibitory effects. Various substituents on nitrogen atom have a different effect on antimicrobial activity. A simple inspection of Table 2 indicated that the presence of sterically bulky groups directly grafted on the nitrogen atom of the benzimidazol-2-ylidene ligand has a positive effect on the antimicrobial activity. Especially, some of the complexes exhibited remarkable inhibitory activity against the growth of bacterial and fungal strains. These results clearly prove the potential of the complexes as antimicrobial drugs. Moreover, further studies focused on the synthesis of new (benz)imidazol-2-ylidene-linked silver complexes, and their biological and medical applications as potential metallopharmaceutical agents are currently underway by our research group. Preliminary catalytic studies revealed that complexes **3a** and **3c** catalyzed the three-component reaction of piperidine, phenylacetylene, and formaldehyde in good yields under neat conditions. Experimental studies on **3a**–**f** complexes were accompanied computationally by DFT when the calculated UV–visible and photoluminescence spectra are in good agreement with the experimental data. TD-DFT

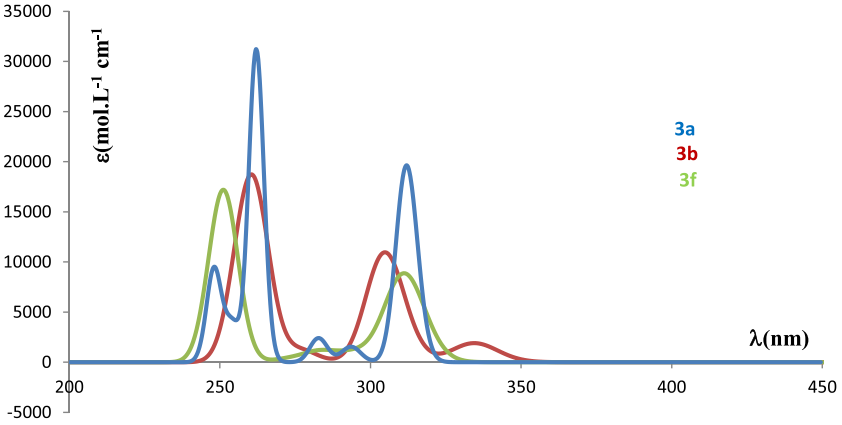

FIGURE 12 UV–visible spectra of the **3a**, **3b**, and **3f** complexes

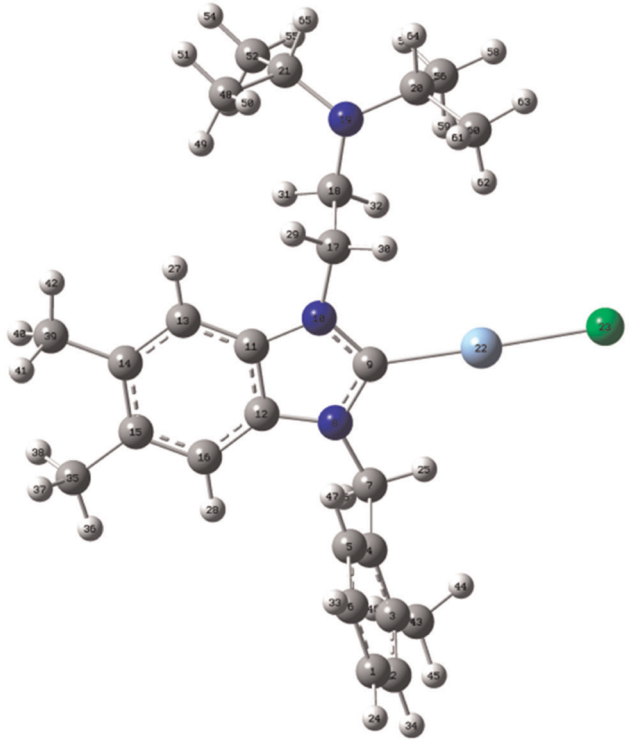

FIGURE 13 Molecular structure of complex **3a**

calculations were also performed to assign the bands observed in the electronic spectra of the **3a**–**f** complexes.

4 | EXPERIMENTAL

4.1 | Chemistry

4.1.1 | General

All reactions were carried out under argon using standard Schlenk line techniques. All chemicals and solvents, including Ag_2O, were purchased from Sigma-Aldrich and Merck. The solvents such as DMF and CH_2Cl_2 were purified by distillation over the drying agents such as phosphorus pentoxide and were transferred under argon atmosphere. Melting points were measured in open capillary tubes with an Electrothermal-9200 melting point apparatus. FTIR spectra were obtained in the range 450–4000 cm^{-1} on a PerkinElmer Spectrum 100 spectrophotometer. ^1H NMR and ^{13}C NMR spectra (see Supporting Information) were recorded using a Bruker Avance AMX and a Bruker Avance III spectrometer operating at 400 MHz (^1H NMR) and at 100 MHz (^{13}C NMR) in $CDCl_3$. The NMR studies were carried out in high-quality 5-mm NMR tubes. The chemical shifts (δ) are reported in ppm, relative to $CDCl_3$. ^1H NMR peaks were labeled as singlet (s), doublet (d), triplet (t), pentet (p), and multiplet (m). ^1H NMR spectra are referenced to residual protiated solvents (δ = 7.26 ppm for $CDCl_3$), and ^{13}C NMR chemical shifts are reported relative to deuterated solvents (δ = 77.16 ppm for $CDCl_3$).

The InChI codes of the investigated compounds are provided as Supporting Information.

Organic solvents (Fluka, puriss) were of spectroscopic grade. UV–vis absorption spectra were recorded on a Shimadzu 1600 spectrophotometer using matched 1-cm quartz cells. Steady-state emission and excitation spectra were recorded using a Jasco FP-8200 spectrofluorometer (Ex bandwidth of 5 nm, Em bandwidth of 5 nm) with a Xe lamp light source. Fluorescence quantum yields (ϕ_f) were measured relative to merocyanine dye[60] in basic media using an absorbance of <0.06 to avoid reabsorption of the emitted light. The following relation has been applied to calculate the fluorescence quantum yields relative to those of the merocyanine dye in basic media[61]:

$$\frac{\phi_f(s)}{\phi_f(r)} = \frac{\int I_s(\bar{\nu})d\bar{\nu}}{I_r(\bar{\nu})d\bar{\nu}} \times \frac{A_r}{A_s} \times \frac{n_s^2}{n_r^2}.$$

The integral represents the corrected fluorescence peak areas, A is the absorbance at the excitation wavelength, n is the solvent refractive index, and the subscripts s and r refer to the sample and reference, respectively.

4.1.2 | Preparation of benzimidazolium salts 2

The reaction of 1-alkyl-benzimidazole (**1a**,**b**) (1 mmol) (**1**) with various alkyl chlorides (1 mmol) in DMF (5 ml) at 80°C for 72 h afforded benzimidazole salts **2a**–**f**. A white crystalline solid was

TABLE 4 A^3 coupling reactions catalyzed by **3a–f**[a]

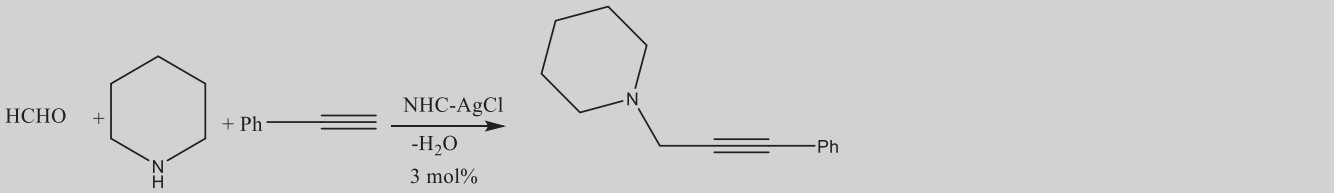

Entry	Catalyst	Solvent	Conversion (%)[b,c]
1	**3a**	Neat	85
2	**3a**	CH_3CN	65
3	**3a**	DMSO	70
4	**3a**	Acetone	45
5	**3a**	DMF	55
6	**3b**	Neat	75
7	**3b**	CH_3CN	55
8	**3c**	Neat	80
10	**3c**	CH_3CN	60
11	**3d**	Neat	80
12	**3d**	CH_3CN	62
13	**3e**	Neat	75
14	**3e**	CH_3CN	45
15	**3f**	Neat	80
16	**3f**	CH_3CN	60

Abbreviations: DMF, dimethylformamide; DMSO, dimethyl sulfoxide.

[a]Reaction conditions: aldehyde (1.0 mmol), amine (1.2 mmol), phenylacetylene (1.5 mmol), catalyst (3 mol %), solvent (2 ml), 18 h, 80°C, in air.

[b]Isolated yields.

[c]Average of two runs.

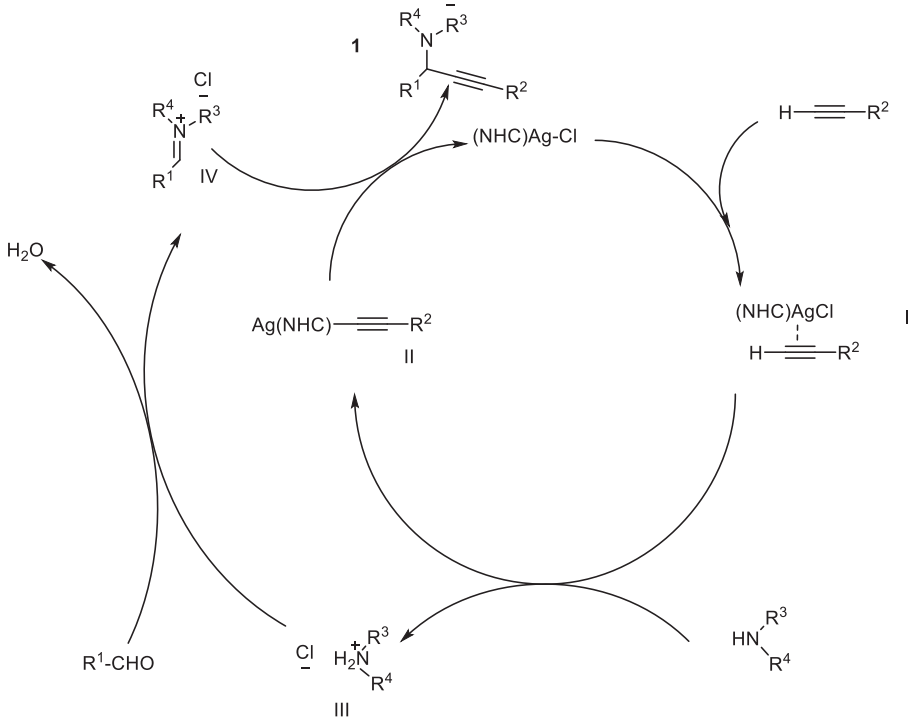

SCHEME 3 The proposed reaction mechanism for NHC–AgCl-catalyzed A^3 coupling reactions

TABLE 5 The antimicrobial activity of the complexes based on the zone of inhibition (zoi) parameter

Microorganism, bacteria/fungi	*Staphylococcus aureus*	*Listeria monocytogenes*	*Escherichia coli*	*Pseudomonas aeruginosa*	*Salmonella typhimurium*	*Candida albicans*
3a	15	16	16	18	18	18
3b	25	20	17	18	20	22
3c	31	30	17	22	28	28
3d	21	25	26	26	–	26
3e	24	16	20	22	18	24
3f	15	18	16	20	18	18
2a	14	15	14	12	22	20
2b	15	16	18	14	22	22
2c	–	–	–	–	–	24
2d	–	12	–	–	16	16
2e	–	–	–	12	15	20
2f	–	–	–	–	15	20
AMC	**16**	**16**	**18**	**20**	**16**	–
Nystatin	–	–	–	–	–	**20**

Abbreviation: AMC, amoxicillin/clavulanic acid.

TABLE 6 Minimal bacterial inhibitory concentration measured in mg/ml of **3a–g**

Microorganisms	Compounds						Ampicillin	Kanamycin
	3a	3b	3c	3d	3e	3f		
Listeria monocytogenes ATCC 19117	3.9	3.9	0.24	15.6	31.25	62.5	3.9	12.5
Staphylococcus aureus	3.9	1.95	0.24	3.9	62.5	125	1.95	6.25
Salmonella typhimurium ATCC 14028	1.95	3.9	0.24	1.95	15.62	62.5	3.9	12.5

obtained after adding diethyl ether (15 ml), which was subsequently filtered off. After washing with diethyl ether (3 × 10 ml), the solid was dried under vacuum and the crude product was recrystallized from dichloromethane/diethyl ether (1:3 ratio).

*1-[2-(Diisopropylamino)ethyl]-3-(2-methylbenzyl)-5,6-dimethylbenzimidazolium chloride (**2a**)*

Yield 75%, Mp: 215°C, ν(CN) = 1549 cm^{-1}. ^{1}H NMR ($CDCl_3$, 400 MHz) δ (ppm) = 0.76 (s, 12H, $CH_{3(a,b,c,d)}$), 2.33 (s, 3H, $CH_{3(e)}$), 2.40 (s, 6H, $CH_{3(f,g)}$), 2.90 (t, 2H, $H_{2'}$), 3.00 (m, 2H, $H_{3'}$, $_{4'}$), 4.54 (t, 2H, $H_{1'}$), 5.77 (s, 2H, $H_{1''}$), 7.15 (m, 5H, $H_{7,3''}$, $_{4'',5'',6''}$), 7.43 (s, 1H, H_4), 11.00 (s, 1H, H_2). ^{13}C NMR ($CDCl_3$, 100 MHz) δ (ppm) = 143.22 (C_2), 136.92 ($C_{2''}$), 136.84 ($C_{3''}$), 136.34 ($C_{5,6}$), 131.14 ($C_{4''}$), 131.112 ($C_{7''}$), 130.22 ($C_{5''}$), 129.83 ($C_{6''}$), 129.04 (C_9), 127.97 (C_8), 113.14 (C_7), 112.89 (C_4), 49.18 ($C_{3'}$, $_{4'}$), 47.61 ($C_{1''}$), 47.18 ($C_{2'}$), 44.10 ($C_{1'}$), 20.69 ($C_{a,b,c,d}$), 19.56 (C_e), 18.52 ($C_{f,g}$). Anal. calc. for $C_{25}H_{36}ClN_3$ (%): C, 72.52; H, 8.76; N, 10.15. Found (%): C, 72.6; H, 8.7; N, 10.2.

*1-[2-(Diisopropylamino)ethyl]-3-(4-methylbenzyl)-5,6-dimethylbenzimidazolium chloride (**2b**)*

Yield 78%, Mp: 220°C, ν(CN) = 1549 cm^{-1}. ^{1}H NMR ($CDCl_3$, 400 MHz) δ (ppm) = 0.75 (s, 12H, $CH_{3(a,b,c,d)}$), 2.27 (s, 3H, H_e), 2.35 (s, 3H, $CH_{3(f)}$), 2.38 (s, 3H, $CH_{3(g)}$), 2.88 (t, 2H, $H_{2'}$), 2.99 (m, 2H, CH $_{(3',4')}$), 4.48 (t, 2H, H_1), 5.71 (s, 2H, $H_{1''}$), 7.12–7.38 (m, 6H, $H_{7,4,2'',3'',5'',6''}$), 11.21 (s, 1H, H_2). ^{13}C NMR ($CDCl_3$, 100 MHz) δ (ppm) = 143.30 (C_2), 136.96 (d, J = 8.4 Hz, $C_{5,6}$), 136.42 ($C_{5''}$), 131.20 ($C_{2''}$), 130.30 (C_9), 129.91 (C_8), 128.05 ($C_{3'',7''}$), 126.73 ($C_{4''}$, $_{6''}$), 113.22 (C_7), 112.97 (C_4), 49.26 ($C_{3',4'}$), 47.69 ($C_{2'}$), 47.26 ($C_{1''}$), 44.18 ($C_{1'}$), 20.77 ($C_{a,b,c,d}$), 19.64 (C_e), 18.52 ($C_{f,g}$). Anal. calc. for $C_{25}H_{36}ClN_3$ (%): C, 72.52; H, 8.76; N, 10.15. Found (%): C, 72.6; H, 8.9; N, 10.1.

*1-[2-(Pyrrolidin-1-yl)ethyl]-3-(2,3,5,6-tetramethylbenzyl)-benzimidazolium chloride (**2c**)*

Yield 70%, Mp: 205°C, ν(CN) = 1559 cm^{-1}. ^{1}H NMR ($CDCl_3$, 100 MHz) δ (ppm) = 1.66 (s, 4H, $H_{5'}$, $_{6'}$), 2.22–2.24 (d, 12H, $CH_{3(a,b,c,d)}$), 2.58 (m, 4H, $H_{4',7'}$), 3.01 (t, 2H, $H_{2'}$), 4.82 (t, 2H, H1′), 5.82 (s, 2H, CH_2, H1″), 7.06–7.79 (m, 5H, $H_{4,5,6,7,5''}$), 10.63 (s, 1H, H_2). ^{13}C NMR

($CDCl_3$, 100 MHz) δ (ppm) = 143.77 (C_2), 135.13 ($C_{2''}$), 134.18 ($C_{4'',6''}$), 133.62 ($C_{3'',7''}$), 131.76 (C_9), 131.34 (C_8), 127.92 ($C_{5''}$), 126.99 (C_5), 126.97 (C_6), 113.53 (C_7), 113.27 (C_4), 53.94 ($C_{4',7'}$), 53.62 ($C_{1''}$), 47.51 ($C_{2'}$), 46.19 ($C_{1'}$), 23.71 ($C_{5',6'}$), 20.67 ($C_{b,c}$), 16.09 ($C_{a,d}$). Anal. calc. for $C_{24}H_{32}ClN_3$ (%): C, 72.43; H, 8.10; N, 10.56. Found (%): C, 72.5; H, 8.2; N, 10.6.

*1-[2-(Pyrrolidin-1-yl)ethyl]-3-(2-methylbenzyl)-5,6-dimetilbenzimidazolium chloride (**2d**)*

Yield 80%, Mp: 240°C, ν(CN) = 1558 cm^{-1}. ^1H NMR ($CDCl_3$, 400 MHz) δ (ppm) = 1.69 (m, 4H, $H_{5',6'}$), 2.29 (s, 3H, $CH_{3(c)}$), 2.35 (s, 3H, $CH_{3(a)}$), 2.38 (s, 3H, $CH_{3(b)}$), 2.61 (m, 4H, $H_{4',7'}$), 3.03 (t, 2H, $H_{2'}$), 4.68 (t, 2H, $H_{1'}$), 5.78 (s, 2H, $H_{1''}$), 7.01–7.46 (m, CH, $H_{4,7,4'',5'',6'',7''}$), 11.19 (s, 1H, H_2). ^{13}C NMR ($CDCl_3$, 100 MHz) δ (ppm) = 143.84 (C_2), 137.45 ($C_{2''}$), 137.37 (C_5), 136.98 (C_6), 131.59 ($C_{3''}$), 131.49 ($C_{4''}$), 130.31 ($C_{7''}$), 130.31 ($C_{5''}$), 129.46 ($C_{6''}$), 128.35 (C_9), 126.97 (C_8), 113.71 (C_7), 113.09 (C_4), 54.36 ($C_{4',7'}$), 54.08 ($C_{1''}$), 50.06 ($C_{2'}$), 46.45 ($C_{1'}$), 24.01 ($C_{5',6'}$), 21.03 (C_a), 19.83 (C_b), 18.82 (C_c). Anal. calc. for $C_{23}H_{30}ClN_3$ (%): C, 71.95; H, 7.88; N, 10.94. Found (%): C, 72.1; H, 7.9; N, 10.8.

*1-[2-(Pyrrolidin-1-yl)ethyl]-3-(2,3,5,6-tetramethylbenzyl)-5,6-dimetilbenzimidazolium chloride (**2e**)*

Yield 85%, Mp: 210°C, ν(CN) = 1560 cm^{-1}. ^1H NMR ($CDCl_3$, 400 MHz) δ (ppm) = 1.72 (m, 4H, $H_{5',6'}$), 2.20 (d, 6H, $CH_{3(a,d)}$), 2.24 (d, 6H, $CH_{3(b,c)}$), 2.34 (s, 3H, $CH_{3(e)}$), 2.40 (s, 3H, $CH_{3(f)}$), 2.72 (m, 4H, $H_{4',7'}$), 3.14 (t, 2H, $H_{2'}$), 4.82 (t, 2H, $H_{1'}$), 5.66 (d, 2H, $H_{1''}$), 7.06 (s, 1H, $H_{5''}$), 7.18 (s, 1H, H_4), 7.64 (s, 1H, H_7), 10.12 (s, 1H, H_2). ^{13}C NMR ($CDCl_3$, 100 MHz) δ (ppm) = 141.62 (C_2), 137.12 ($C_{2''}$), 137.00 (C_5), 134.83 (C_6), 133.83 ($C_{4'',6''}$), 133.29 ($C_{3'',7''}$), 129.87 (C_9), 129.52 (C_8), 127.50 ($C_{5''}$), 112.82 (C_7), 112.72 (C_4), 53.45 ($C_{4',7'}$), 52.86 ($C_{1''}$), 46.63 ($C_{2'}$), 45.18 ($C_{1'}$), 23.31 ($C_{5',6'}$), 20.40–20.32 ($C_{b,c}$), 18.20 ($C_{e,f}$), 15.73 ($C_{a,d}$). Anal. calc. for $C_{26}H_{36}ClN_3$ (%): C, 73.30; H, 8.52; N, 9.86. Found (%): C, 73.1; H, 8.5; N, 9.8.

*1-[2-(Pyrrolidin-1-yl)ethyl]-3-(2,3,4,5,6-pentamethylbenzyl)-benzimidazolium chloride (**2f**)*

Yield 67%, Mp: 215°C, ν(CN) = 1560 cm^{-1}. ^1H NMR ($CDCl_3$, 400 MHz) δ (ppm) = 1.75 (m, 4H, $H_{5',6'}$), 2.25 (s, 6H, $CH_{3(a,e)}$), 2.28 (s, 9H, $CH_{3(b,c,d)}$), 2.78 (m, 4H, $H_{4',7'}$), 3.20 (s, 2H, $H_{2'}$), 4.95 (s, 2H, $H_{1'}$), 5.76 (s, 2H, $H_{1''}$), 7.94–7.43 (m, 4H, $H_{4,5,6,7}$), 10.47 (s, 1H, H_2). ^{13}C NMR ($CDCl_3$, 100 MHz) δ (ppm) = 143.12 (C_2), 137.38 ($C_{2''}$), 133.96 (C_9), 133.57 (C_8), 131.71 ($C_{3'',7''}$), 131.22 ($C_{4'',6''}$), 127.13 (d, J = 13.2 Hz, $C_{5,6}$), 124.91 ($C_{5''}$), 113.43 (d, J = 18.1 Hz, $C_{7,4}$), 53.70 ($C_{4',7'}$), 53.16 ($C_{2'}$), 47.77 ($C_{1''}$), 45.52 ($C_{1'}$), 23.55 ($C_{5',6'}$), 17.34 ($C_{a,e}$), 17.02 (d, J = 1.8 Hz, $C_{b,c,d}$). Anal. calc. for $C_{25}H_{34}ClN_3$ (%): C, 72.88; H, 8.32; N, 10.20. Found (%): C, 72.8; H, 8.4; N, 10.3.

4.1.3 | General procedure for the preparation of silver(I)–NHC complexes **3a–f**

A solution of benzimidazolium salt (1.0 mmol) (**2a–f**) and Ag_2O (1.4 mmol) in dichloromethane (15 ml) was stirred for 120 h at room temperature in the dark. The reaction mixture was filtered through celite and the solvent was removed under reduced pressure. The crude product was recrystallized from dichloromethane/diethyl ether (1:3).

*Chloro-{1-[2-(diisopropylamino)ethyl]-3-(2-methylbenzyl)-5,6-dimethylbenzimidazole-2-ylidene}silver(I) (**3a**)*

Yield 75%, Mp: 185°C, ν(CN) = 1484 cm^{-1}. ^1H NMR ($CDCl_3$, 400 MHz) δ (ppm) = 0.94 (s, 12H, $CH_{3(a,b,c,d)}$), 2.29 (s, 3H, $CH_{3(e)}$), 2.40 (s, 6H, $CH_{3(f,g)}$), 2.90 (t, 2H, $H_{2'}$), 3.04 (m, 2H, $H_{3',4'}$), 4.33 (t, 2H, $H_{1'}$), 5.51 (t, 2H, $H_{1''}$), 7.24–6.61 (m, 6H, $H_{7,4,4'',5'',6'',7''}$). ^{13}C NMR ($CDCl_3$, 100 MHz) δ (ppm) = 134.00 ($C_{2''}$), 133.48 ($C_{7''}$), 133.28 ($C_{5,6}$), 131.24 ($C_{6''}$), 128.44 ($C_{9,8}$), 128.24 ($C_{3''}$), 126.91 ($C_{4'',5''}$), 112.55 (C_7), 112.34 (C_8), 51.50 ($C_{4',3'}$), 51.07 ($C_{1''}$), 49.17 ($C_{2'}$), 46.00 ($C_{1'}$), 21.41 ($C_{a,b,c,d}$), 20.94 (C_e), 20.73 (C_f), 19.96 (C_g). Anal. calc. for $C_{25}H_{35}AgClN_3$ (%): C, 57.65; H, 6.77; N, 8.07. Found (%): C, 57.7; H, 6.75; N, 8.1.

*Chloro-{1-[2-(diisopropylamino)ethyl]-3-(4-methylbenzyl)-5,6-dimethylbenzimidazole-2-ylidene}silver(I) (**3b**)*

Yield 78%, Mp: 290°C, ν(CN) = 1445 cm^{-1}. ^1H NMR ($CDCl_3$, 400 MHz) δ (ppm) = 0.93 (s, 12H, $CH_{3(a,b,c,d)}$), 2.31 (s, 6H, $CH_{3(f,g)}$), 2.37 (s, 3H, $CH_{3(e)}$), 2.88 (t, 2H, $H_{2'}$), 3.02 (m, 2H, $H_{3',4'}$), 4.31 (t, 2H, $H_{1'}$), 5.49 (s, 2H, $H_{1''}$), 7.07–7.22 (m, 6H, $H_{4,7,3'',4'',6'',7''}$). ^{13}C NMR ($CDCl_3$, 100 MHz) δ (ppm) = 138.33 ($C_{2''}$), 133.56 ($C_{5''}$), 133.50 ($C_{5,6}$), 132.36 ($C_{9,8}$), 129.79 ($C_{4'',6''}$), 127.23 ($C_{3'',7''}$), 112.30 (C_7), 111.96 (C_4), 53.16 ($C_{3',4'}$), 50.68 ($C_{1''}$), 48.96 ($C_{1'}$), 45.68 ($C_{2'}$), 21.08 ($C_{a,b,c,d}$), 20.60 (C_e), 20.57 ($C_{f,g}$). Anal. calc. for $C_{25}H_{35}AgClN_3$ (%): C, 57.65; H, 6.77; N, 8.07. Found (%): C, 57.7; H, 6.75; N, 8.1.

*Chloro-{1-[2-(pyrrolidin-1-yl)ethyl]-3-(2,3,5,6-tetrabenzyl)-benzimidazole-2-ylidene}silver(I) (**3c**)*

Yield 80%, Mp: 180°C, ν(CN) = 1473 cm^{-1}. ^1H NMR ($CDCl_3$, 400 MHz) δ (ppm) = 1.74 (m, 4H, $H_{5',6'}$), 2.13 (s, 6H, $CH_{3(a,d)}$), 2.28 (s, 6H, $CH_{3(b,c)}$), 2.56 (m, 4H, $H_{4',7'}$), 2.90 (t, 2H, $H_{2'}$), 4.45 (t, 2H, $H_{1'}$), 5.46 (s, 2H, $H_{1''}$), 7.12–7.51 (m, 5H, $H_{4,5,6,7,5''}$). ^{13}C NMR ($CDCl_3$, 100 MHz) δ (ppm) = 135.06 ($C_{2''}$), 134.04 ($C_{4'',6''}$), 133.57 ($C_{3'',7''}$), 133.27 (C_8), 132.91 (C_9), 129.50 ($C_{5''}$), 124.06 (C_5), 123.84 (C_6), 111.19 (C_7), 111.17 (C_4), 55.56 ($C_{4',7'}$), 54.23 ($C_{2'}$), 49.03 ($C_{1''}$), 47.24 ($C_{1'}$), 23.37 ($C_{5',6'}$), 20.46 ($C_{b,c}$), 15.94 ($C_{a,d}$). Anal. calc. for $C_{24}H_{31}AgClN_3$ (%): C, 57.10; H, 6.19; N, 8.32. Found (%): C, 57.2; H, 6.3; N, 8.4.

*Chloro-{1-[2-(pyrrolidin-1-yl)ethyl]-3-(2-methylbenzyl)-5,6-dimethylbenzimidazole-2-ylidene}silver(I) (**3d**)*

Yield 70%, Mp: 200°C, ν(CN) = 1486 cm^{-1}. ^1H NMR ($CDCl_3$, 400 MHz) δ (ppm) = 1.79 (m, 4H, $H_{5',6'}$), 2.28 (s, 3H, $CH_{3(a)}$), 2.37 (s, 6H, $CH_{3(b,c)}$), 2.62 (m, 4H, $H_{4',7'}$), 2.96 (t, 2H, $H_{2'}$), 4.49 (t, 2H, $H_{1'}$), 5.51 (s, 2H, $H_{1''}$), 7.06–7.29 (m, 6H, $H_{7,4,4'',5'',6'',7''}$). ^{13}C NMR ($CDCl_3$, 100 MHz) δ (ppm) = 135.45 ($C_{2''}$), 133.85 ($C_{3''}$), 133.81 (C_9), 133.18 (C_8), 132.53 ($C_{4''}$), 130.93, 188.26 (C_2), ($C_{7''}$), 128.31 (C_5), 126.61 (C_6), 126.32 ($C_{5'',6''}$), 112.29 (C_7), 111.73 (C_4), 55.97 ($C_{4'}$), 54.70 ($C_{7'}$), 51.24 ($C_{2'}$), 48.78 ($C_{1''}$), 23.74 ($C_{1'}$), 20.51 ($C_{5',6'}$), 19.65 ($C_{a,b,c}$). Anal. calc. for $C_{23}H_{29}AgClN_3$ (%): C, 56.28; H, 5.96; N, 8.56. Found (%): C, 56.3; H, 6.1; N, 8.6.

*Chloro-{1-[2-(pyrrolidin-1-yl)ethyl]-3-(2,3,5,6-tetramethylbenzyl)-5,6-dimethylbenzimidazole-2-ylidene}silver(I) (**3e**)*

Yield 75%, Mp: 212°C, ν(CN) = 1474 cm^{-1}. ^1H NMR ($CDCl_3$, 400 MHz) δ (ppm) = 1.76–1.73 (m, 4H, $H_{5',6'}$), 2.12 (s, 6H, $CH_{3(c,b)}$), 2.29 (s, 6H, $CH_{3(a,d)}$), 2.39–2.40 (d, J = 5.3 Hz, 6H, $CH_{3(e,f)}$), 2.58–2.54 (m, 4H, $H_{4',7'}$), 2.89–2.85 (t, 2H, $H_{2'}$), 4.42–4.38 (t, 2H, $H_{1'}$), 5.38 (s, 2H, $H_{1''}$), 7.13 (s, 1H, $H_{5''}$), 7.21 (s, 1H, H_7), 7.27 (s, 1H, H_4). ^{13}C NMR ($CDCl_3$, 100 MHz) δ (ppm) = 135.40 ($C_{2''}$), 133.80 ($C_{4'',6''}$), 133.60 ($C_{3'',7''}$), 133.45 (C_5), 133.18 (C_6), 133.04 (C_9), 132.41 (C_8), 130.05 ($C_{5''}$), 111.69 (d, J = 8.6 Hz, $C_{7,4}$), 188.04 (C_2), 54.55 ($C_{3',7'}$), 49.35 ($C_{1''}$), 47.12 ($C_{1'}$), 23.71 ($C_{5',6'}$), 20.82 ($C_{b,c}$) 20.63 ($C_{e,f}$), 16.26 ($C_{a,d}$). Anal. calc. for $C_{26}H_{35}AgClN_3$ (%): C, 58.60; H, 6.62; N, 7.89. Found (%): C, 58.7; H, 6.70; N, 7.9.

*Chloro-{1-[2-(pyrrolidin-1-yl)ethyl]-3-(2,3,4,5,6-pentamethylbenzyl)-benzimidazole-2-ylidene}silver(I) (**3f**)*

Yield 85%, Mp: 185°C, ν(CN) = 1478 cm^{-1}. ^1H NMR ($CDCl_3$, 400 MHz) δ (ppm) = 1.77–1.73 (m, 4H, $H_{5',6'}$), 2.19 (s, 6H, $CH_{3(a,e)}$), 2.28 (s, 6H, $CH_{3(b,d)}$), 2.33 (s, 3H, $CH_{3(c)}$), 2.56 (m, 4H, $H_{4',7'}$), 2.92–2.87 (t, 2H, $H_{2'}$), 4.48–4.44 (t, 2H, $H_{1'}$), 5.47 (s, 2H, $H_{1''}$), 7.41 (m, 2H, $H_{5,6}$), 7.47 (d, J = 6.7 Hz, 1H, CH, H_7), 7.53 (d, J = 8.4 Hz, 1H, CH, H_4). ^{13}C NMR ($CDCl_3$, 100 MHz) δ (ppm) = 137.43 ($C_{2''}$), 134.42 ($C_{3'',7''}$), 134.36 (C_9), 134.07 (C_8), 133.09 ($C_{4'',6''}$), 126.73 ($C_{5''}$), 124.40 (C_5), 124.10 (C_6), 111.52 (d, J = 5.0 Hz, $C_{7,4}$), 55.99 ($C_{2'}$), 54.59 ($C_{4',7'}$), 49.45 ($C_{1''}$), 47.91 ($C_{1'}$), 23.73 ($C_{5',6'}$), 17.54 (C_c), 17.28 (d, J = 2.5 Hz, $C_{a,b,d,e}$). Anal. calc. for $C_{25}H_{33}AgClN_3$ (%): C, 57.87; H, 6.41; N, 8.10. Found (%): C, 57.9; H, 6.5; N, 8.2.

4.1.4 | General procedure for the Ag(I)–NHC-catalyzed three-component coupling reaction

In a typical procedure, a mix of phenylacetylene (1.5 mmol, 164.7 ml), aldehyde (1.0 mmol), piperidine (1.2 mmol, 118.7 ml), and silver complex (3 mol%) was added to an oven-dried Schlenk tube (15 ml) with 1,4-dioxane (2.0 ml). The Schlenk tube was placed in a pre-heated oil bath (80°C). The mixture was stirred at 80°C for a given time under an argon atmosphere. After the reaction was completed, the mixture was cooled to room temperature and diethyl ether was added. The organic portion was dried over $MgSO_4$ and filtered. After the volatile components were removed in a vacuum, the residue was purified by column chromatography on silica using ethyl acetate/hexane (1:2).

4.2 | Biological assays

4.2.1 | Bacterial strains, media, and growth conditions

Microorganisms defined in the American Type Culture Collection (ATCC) were used in antimicrobial studies. Mueller–Hinton Broth was purchased from HiMedia Laboratories Pvt. Ltd. and RPMI-1640 broth was purchased from Sigma-Aldrich (Chemie GmbH).

The bacterial strains used as indicator microorganisms for the antibacterial activity assays were *M. luteus* LB 14110, *S. aureus* ATCC 6538, *L. monocytogenes* ATCC 19117, *S. typhimurium* ATCC 14028, *P. aeruginosa* ATCC 49189, and *E. coli*, which were obtained from International Culture Collections (ATCC) and local culture collection of the Laboratory of Microorganisms and Biomolecules of the Centre of Biotechnology of Sfax, Tunisia.

These bacterial strains were grown overnight in Luria–Bertani (LB) agar medium (g/l), containing peptone 10, yeast extract 5, and NaCl 5, at pH 7.2 under aerobic conditions and constant agitation (200 rpm) at 30°C for *M. luteus* LB14110 and *L. monocytogenes* ATCC 19117 and at 37°C for *S. aureus* ATCC 6538, *S. typhimurium* ATCC 14028, and *P. aeruginosa* ATCC 49189, and then diluted, 1:100, in LB media and incubated for 5 h under constant agitation (200 rpm) at the appropriate temperature.

4.2.2 | Agar well diffusion method

The agar well diffusion method was employed for the determination of the antimicrobial activity of the synthesized compounds according to Güven et al.,[62] with some modifications. Briefly, the synthesized compounds were allowed to diffuse out into the appropriate agar medium (LB agar medium) and interact in a plate freshly seeded with a suspension of the indicator microorganisms (0.1 ml of 10^8 cells per ml). The plate was incubated at the appropriate temperature after allowing to stand at 4°C for 2 h. The resulting zones of inhibition would be uniformly circular as there would be a confluent lawn of growth. The antibacterial activity was assayed by measuring the diameter of the inhibition zone formed around the well in millimeters. All tests were assayed in triplicate and expressed as the average ± *SD* of the measurements.

4.2.3 | MIC

The MIC of the synthesized compounds was determined by NCCLS guidelines M7-A6 and M38-P (National Committee for Clinical Laboratory Standard, Wayne 1998).[63] The test was performed in sterile 96-well microplates with a final volume of 100 µl in each microplate well. The synthesized compounds (20 mg/ml) were properly prepared in a solution of DMSO/water (1/9; v/v). The inhibitory activity of each synthesized compound was transferred to each well to obtain a two fold serial dilution of the original sample. As an indicator of microorganism growth, 25 µl of thiazolyl blue tetrazolium bromide (MTT) indicator solution (0.5 mg/ml) dissolved in sterile water was added to the wells and incubated at room temperature for 30 min. This determination was performed in triplicate, and the obtained results were very similar. The reported value is the average of the three tests.

ACKNOWLEDGMENTS

This study was supported by the İnönü University Research Fund (iÜ-BAP: FBG-2019-1594).

ORCID

Naceur Hamdi https://orcid.org/0000-0003-0110-9588

REFERENCES

[1] M. N. Hopkinson, C. Richter, M. Schedler, F. Glorius, *Nature* **2014**, *510*(*7506*), 485.
[2] T. Roth, V. Vasilenko, C. G. M. Benson, H. Wadepohl, D. S. Wright, L. H. Gade, *Chem. Sci.* **2015**, *4*, 2506.
[3] N. Wang, J. Xu, J. K. Lee, *Org. Biomol. Chem.* **2018**, *37*, 8230.
[4] V. Nesterov, D. Reiter, P. Bag, P. Frisch, R. Holzner, A. Porzelt, S. Inoue, *Chem. Rev.* **2018**, *19*, 9678.
[5] Y. Liu, X. Zhang, R. Zeng, Y. Zhang, Q. S. Dai, H. J. Leng, X. J. Gou, J. L. Li, *Molecules* **2017**, *11*, 1882.
[6] B. S. Yun, J. H. Kim, S. Y. Kim, H. J. Son, D. W. Cho, S. O. Kang, *Phys. Chem. Chem. Phys.* **2019**, *13*, 7155.
[7] N. M. Scott, S. P. Nolan, *Eur. J. Inorg. Chem.* **2005**, *10*, 1815.
[8] C. J. Collett, R. S. Massey, J. E. Taylor, O. R. Maguire, A. C. O'Donoghue, A. D. Smith, *Angew. Chem. Weinheim. Bergstr. Ger.* **2015**, *23*, 6991.
[9] C. K. Chung, R. H. Grubbs, *Org. Lett.* **2008**, *13*, 2693.
[10] D. W. Woolley, *J. Biol. Chem.* **1944**, *2*, 225.
[11] M. T. Khan, M. T. Razi, S. U. Jan, M. Mukhtiar, R. Gul, U. Izhar, A. Hussain, A. M. Hashmi, M. T. Ahmad, N. A. Shahwani, I. R., Pak, *J. Pharm. Sci.* **2018**, *3*, 1067.
[12] G. Kaur, O. Silakari, *Bioorg. Chem.* **2018**, *80*, 24.
[13] F. F. Al-Blewi, M. A. Almehmadi, M. R. Aouad, S. K. Bardaweel, P. K. Sahu, M. Messali, N. Rezki, E. S. H. El Ashry, *Chem. Cent. J.* **2018**, *1*, 110.
[14] H. L. Kuo, J. C. Lien, C. H. Chung, C. H. Chang, S. C. Lo, I. C. Tsai, H. C. Peng, S. C. Kuo, T. F. Huang, *Naunyn-Schmiedeberg's Arch. Pharmacol.* **2010**, *6*, 495.
[15] B. Da Silva, M. Habibi, S. Ognier, G. Schelcher, J. Mostafavi-Amjad, H. R. M. Khalesifard, D. Bonn, *Eur. Phys. J.: Spec. Top.* **2016**, *4*, 707.
[16] (a) C. G. Hartinger, P. J. Dyson, *Chem. Soc. Rev.* **2009**, *2*, 391.; (b) W. Liu, R. Gust, *Chem. Soc. Rev.* **2013**, *2*, 755.
[17] S. Ajay, P. P. Saidhareddy, A. K. Shaw, *Asian J. Org. Chem.* **2017**, *6*, 503.
[18] V. Panwar, S. L. Jain, *Mater. Sci. Eng. C* **2019**, *99*, 191.
[19] S. Dapeng, D. Zhongyu, *Chin. J. Org. Chem.* **2020**, *40*, 1316.
[20] H. N. K. Lam, N. B. Nguyen, G. H. Dang, T. Truong, N. T. S. Phan, *Catal. Lett.* **2016**, *146*, 2087.
[21] A. D. Russel, F. R. C. Path, W. B. Hugo, *Prog. Med. Chem.* **1994**, *31*, 351.
[22] C. A. Moyer, L. Brentanol, D. L. Gravens, H. W. Margraf, W. W. Monafo, *Arch. Surg.* **1965**, *90*, 812.
[23] C. L. Fox, *Arch. Surg.* **1968**, *96*, 184.
[24] A. B. J. Lansdown, *J. Wound Care* **2002**, *11*, 125.
[25] S. Silver, *FEMS Microbiol. Rev.* **2003**, *27*, 341.
[26] W. J. Youngs, A. R. Knapp, P. O. Wagers, C. A. Tessier, *Dalton Trans.* **2012**, *41*, 327.
[27] A. Melaiye, R. S. Simons, A. Milsted, F. Pingitore, C. Wesdemiotis, C. A. Tessier, W. J. Youngs, *J. Med. Chem.* **2004**, *47*, 973.
[28] A. Melaiye, Z. Sun, K. Hindi, A. Milsted, D. Ely, D. H. Reneker, C. A. Tessier, W. J. Youngs, *J. Am. Chem. Soc.* **2005**, *127*, 2285.
[29] A. Kascatan-Nebioglu, A. Melaiye, K. Hindi, S. Durmus, M. J. Panzner, L. A. Hogue, R. J. Mallett, C. E. Hovis, M. Coughenour, S. D. Crosby, A. Milsted, D. L. Ely, C. A. Tessier, C. L. Cannon, J. Youngs, *J. Med. Chem.* **2006**, *49*, 6811.
[30] K. M. Hindi, T. J. Siciliano, S. Durmus, M. J. Panzner, D. A. Medvetz, D. V. Reddy, L. A. Hogue, C. E. Hovis, J. K. Hilliard, R. J. Mallet, C. A. Tessier, C. L. Cannon, W. J. J. Youngs, *Med. Chem.* **2008**, *51*, 1577.
[31] M. J. Panzner, K. M. Hindi, B. D. Wright, J. B. Taylor, D. S. Han, Youngs, W. J. C. L. Cannon, *Dalton Trans.* **2009**, *35*, 7308.
[32] R. A. Haque, M. A. Iqbal, F. Mohamad, M. R. Razali, *J. Mol. Struct.* **2018**, *1155*, 362.
[33] R. X. Zhao, J. Wang, D. W. Jing, H. J. Zhang, C. Feng, G. Y. Li, *Inorg. Chem. Commun.* **2019**, 107597.
[34] S. H. Alisir, B. Sariboga, S. Caglar, O. Buyukgungor, *J. Mol. Struct.* **2017**, *1130*, 156.
[35] R. A. Haque, M. A. Iqbal, S. Budagumpi, M. B. Khadeer Ahamed, A. M. Abdul Majid, N. Hasanudin, *App. Organomet. Chem.* **2013**, *4*, 214.
[36] (a) K. M. Hindi, M. J. Panzner, C. A. Tessier, C. L. Cannon, W. J. Youngs, *Chem. Rev.* **2009**, *109*, 3859.; (b) M. Tacke, *J. Organomet. Chem.* **2015**, *782*, 17.; (c) T. Samanta, R. N. Munda, G. Roymahapatra, A. Nandy, K. D. Saha, S. S. Al-Deyab, J. Dinda, *J. Organomet. Chem* **2015**, *791*, 183.
[37] (a) R. A. Haque, S. Y. Choo, S. Budagumpi, M. A. Iqbal, A. A. Abdullah, *Eur. J. Med. Chem.* **2015**, *90*, 82.; (b) M. O. Karataş, B. Olgundeniz, S. Günal, İ. Özdemir, B. Alıcı, E. Çetinkaya, *Bioorg. Med. Chem.* **2016**, *24*, 643.
[38] (a) C. R. Shahini, G. Achar, S. Budagumpi, H. Müller-Bunz, M. Tacke, S. A. Patil, *J. Organomet. Chem.* **2018**, *868*, 1.; (b) C. O'Beirne, N. F. Alhamad, Q. Ma, H. Müller-Bunz, K. Kavanagh, G. Butler, X. Zhu, M. Tacke, *Inorg. Chim. Acta* **2019**, *486*, 294.
[39] (a) A. Hecel, P. Kolkowska, K. Krzywoszynska, A. Szebesczyk, M. Rowinska-Zyrek, H. Kozlowski, *Curr. Med. Chem.* **2019**, *26*, 624.; (b) R. Ashraf, H. N. Bhatti, M. A. Iqbal, Y. Jamil, *Inorg. Chem. Commun.* **2020**, *119*, 108077.; (c) O. E. Palomero, A. L. Cunningham, B. W. Davies, R. A. Jones, *Inorg. Chim. Acta* **2021**, *517*, 120152.
[40] D. J. Nielsen, K. J. Cavell, B. W. Skelton, A. H. White, *Inorg. Chim. Acta* **2003**, *352*, 143.
[41] J. Pytkowicz, S. Roland, P. Mangeney, *J. Organomet. Chem.* **2001**, *631*, 157.
[42] H. M. Lee, P. L. Chiu, C. H. Hu, C. L. Lai, Y. C. Chou, *J. Organomet. Chem.* **2005**, *690*, 403.
[43] I. Slimani, A. C. Mtiba, L. Mellouli, L. Mansour, I. Özdemir., N. Gürbüz, N. Hamdi, *J. Braz. Chem. Soc.* **2020**, *10*, 2058.
[44] İ. Özdemir,O. Çiftçi, E. Evren, N. Gürbüz, N. Kaloğlu, N. B. Türkmen, Ş. Yaşar, E. Üstün, N. Hamdi, L. Mansour, İ. Özdemir, *Inorg. Chim. Acta.* **2020**, *506*, 119530.
[45] Gaussian 09, Revision A.1, M. J. Frisch, G. W. Trucks, H. B. Schlegel, G. E. Scuseria, M. A. Robb, J. R. Cheeseman, G. Scalmani, V. Barone, B. Mennucci, G. A. Petersson, H. Nakatsuji, M. Caricato, X. Li, H. P. Hratchian, A. F. Izmaylov, J. Bloino, G. Zheng, J. L. Sonnenberg, M. Hada, M. Ehara, K. Toyota, R. Fukuda, J. Hasegawa, M. Ishida, T. Nakajima, Y. Honda, O. Kitao, H. Nakai, T. Vreven, J. A. Montgomery, Jr., J. E. Peralta, F. Ogliaro, M. Bearpark, J. J. Heyd, E. Brothers, K. N. Kudin, V. N. Staroverov, R. Kobayashi, J. Normand, K. Raghavachari, A. Rendell, J. C. Burant, S. S. Iyengar, J. Tomasi, M. Cossi, N. Rega, J. M. Millam, M. Klene, J. E. Knox, J. B. Cross, V. Bakken, C. Adamo, J. Jaramillo, R. Gomperts, R. E. Stratmann, O. Yazyev, A. J. Austin, R. Cammi, C. Pomelli, J. W. Ochterski, R. L. Martin, K. Morokuma, V. G. Zakrzewski, G. A. Voth, P. Salvador, J. J. Dannenberg, S. Dapprich, A. D. Daniels, O. Farkas, J. B. Foresman, J. V. Ortiz, J. Cioslowski, D. J. Fox, *Gaussian Inc., Wallingford, CT*, **2009**.
[46] M. A. Ben Aissa, S. Hassen, Y. Arfaoui, *Int. J. Quantum Chem.* **2020**, *6*, 25837.
[47] Y. L. Li, L. Han, Y. Mei, J. Z. H. Zhang, *Chem. Phys. Lett.* **2009**, *482*, 217.
[48] J. Aihara, *Phys. Chem. Chem. Phys.* **2000**, *2*, 3121.

[49] J. Ralph, G. Pearson, *Chem. Sci.* **2005**, *5*, 369.
[50] S. Hassen, H. Chebbi, M. F. Zid, Y. Arfaoui, *J. Mol. Struct.* **2019**, *1179*, 678.
[51] V. A. Peshkov, O. P. Pereshivko, E. V. Van der Eycken, *Chem. Soc. Rev.* **2012**, *41*, 3790.
[52] S. Sakaguchi, T. Kubo, Y. Ishii, *Angew. Chem. Int. Ed.* **2001**, *40*, 2534.
[53] C. M. Wei, Z. G. Li, C. J. Li, *Org. Lett.* **2003**, *5*, 4473.
[54] R. Manikandan, P. Anitha, P. Viswanathamurthi, J. G. Malecki, *Polyhedron* **2016** *119*, 300.
[55] L. Shi, Y. Q. Tu, M. Wang, F. M. Zhang, C. A. Fan, *Org. Lett.* **2004**, *6*, 1001.
[56] L. Rubio-Perez, M. Iglesias, J. Munarriz, V. Polo, J. J. Perez-Torrente, L. A. Oro, *Chem.–Eur. J.* **2015**, *21*, 17701.
[57] R. Kilincarslan, A. Kunduracioglu, N. Sadic, *Rev. Chim.* **2016**, *67*, 2214.
[58] P. Li, L. Wang, Y. Zhang, M. Wang, *Tetrahedron Lett.* **2008**, *49*, 6650.
[59] I. Slimani, L. Mansour, N. Abutaha, A. Halim Harrath, J. Al-Tamimi, N. Gürbüz, I. Özdemir, N. Hamdi, *J. King Saud Univ.* **2020**, *32*, 1544.
[60] J. Jentzsch, W. S. Koko, I. Al Nasr, T. A. Khan, R. Schobert, K. Ersfeld, B. Biersack, *Chem. Biodivers.* **2019**, *2*, 17.
[61] M. H. Abdel-Kader, U. Steiner, *J. Chem. Educ.* **1983**, *60*, 160.
[62] J. N. Demas, G. A. Crosby, *J. Phys. Chem.* **1971**, *75*, 1001.
[63] J. R. Tagg, A. R. McGiven, *App Microbiol.* **1971**, *21*, 943.

SUPPORTING INFORMATION

Additional Supporting Information may be found online in the supporting information tab for this article.

How to cite this article: A. Mnasri, A. Mejri, S. M. Al-Hazmy, Y. Arfaoui, I. Özdemir, N. Gürbüz, N. Hamdi. Silver–*N*-heterocyclic carbene complexes-catalyzed multicomponent reactions: Synthesis, spectroscopic characterization, density functional theory calculations, and antibacterial study. *Arch. Pharm.* 2021;e2100111.
https://doi.org/10.1002/ardp.202100111